# Optimal Operation of Distillation Processes under Uncertain Inflows Accumulated in a Feed Tank

**Pu Li, Moritz Wendt, H. Arellano-Garcia, Günter Wozny**
Institut für Prozess und Anlagentechnik, Technische Universität Berlin, KWT 9
10623 Berlin, Germany

*A new method of optimizing the operation of distillation processes with uncertain inflow streams from upstream plants is discussed. The case considered is the streams that will be first accumulated in a tank before feeding to the column. To minimize the total amount of operating energy while keeping a stable column operation under these inflows, a novel decomposed optimization strategy consisting of two steps was used. For an optimal planning of the dynamic operation, a smooth feed flow policy to the column is developed in the first step by stochastic optimization under chance constraints by ensuring a predefined probability of holding the tank level inside the desired range. An easy-to-use method developed computes the maximum reachable probability of holding the constraints so that a feasible solution of the chance constrained problem can be guaranteed. Since the uncertainty in the inflow stream variability is absorbed in the stochastic optimization over the tank, the operation of the dowstream distillation column is deterministic. Therefore, in the second step, the reflux and reboiler duty policies of the column are developed by deterministic dynamic optimization. The optimal overall strategy is obtained by the maximized smoothness of the feed flow to the distillation column. The approach is applied to a pilot column, and the developed operating policies are implemented on the real plant by experiment.*

## Introduction

Optimization is an important way to enhance the profit and reduce the environmental impact of industrial processes by exploiting the degree of freedom. Studies on dynamic optimization have been emphasized recently for optimal design and operation of increasingly intensified processes. Deterministic nonlinear optimization methods have been developed for solving large-scale nonlinear programming (NLP) problems (Gill et al., 1997; Leineweber et al., 1997). Approaches to solve dynamic optimization problems usually use a discretization method to transform the dynamic system to a NLP problem. They can be classified into simultaneous approaches (Steinbach, 1995; Cervantes and Biegler, 1998), where all discretized variables are included in a huge NLP problem, and sequential approaches (Logsdon and Biegler, 1992; Vassiliadis et al., 1994; Li, 1998; Feehery and Barton, 1998), where a simulation step is used to compute the dependent variables and thus only the independents are solved by NLP. Although these approaches have been successfully applied to many chemical plants such as reactive, azeotropic, and batch distillation processes (Logsdon and Biegler, 1989; Li et al., 1998; Wendt et al., 2000), the optimization results are only applicable when the real operating conditions are included in the optimization.

### *Optimization under uncertainty*

To deal with the unknown operating reality *a priori*, optimization under uncertainty has to be considered. A process may have internal uncertainties such as inaccurate model parameters or structures and external uncertainties such as unknown future feedstock or atmospheric temperature. Many

Correspondence concerning this article should be addressed to P. Li.

previous studies on the optimal process *design* under model uncertainty have been made. These studies may also be classified into two approaches in view of treating the uncertainties: (i) discretization approaches (Halemane and Grossmann, 1983; Varvarezos et al., 1992; Subrahmanyam et al., 1994; Pistikopoulos and Ierapetritou, 1995; Bhatia and Biegler, 1997; Rooney and Biegler, 1999) and (ii) multivariate integration approaches (Diwekar and Rubin, 1991; Clay and Grossmann, 1997; Diwekar and Kalagnannam, 1997; Bernado et al., 1999). In the former approaches the bounded uncertain parameters will be discretized into multiple intervals such that each individual interval represents a scenario with an approximated discrete distribution. This leads to a multiperiod optimization problem that provides the solution which is feasible only on the selected points. Thus, the feasibility problem is then tested over the entire range of parameters. The latter approaches consider the continuous stochastic distribution of the uncertain parameters with the probability density function. In these approaches, a multivariate numerical integration scheme will be chosen. An approximated integration through a sampling scheme and a rigorous direct integration are the two integration methods used in the literature.

To solve an optimization problem under uncertainty, some special treatments to the objective function, and the equality and inequality constraints have to be considered in order to relax the stochastic problem to an equivalent NLP problem so that it can be solved by the existing optimization routines. Minimizing the expected value of the objective function has been usually adopted (Torvi and Herzberg, 1997; Acevedo and Pistikopoulos, 1998). To handle the inequality constraints under uncertainty, recourse and chance constraints are the two main approaches used (Prékopa, 1995). In the approach of *recourse*, violations of the constraints are allowed and will be compensated by introducing a penalty term in the objective function. This approach is very suitable to solving process planning problems under demand uncertainty (Subrahmanyam et al., 1994; Liu and Sahinidis, 1996; Ahmed and Sahinidis, 1998; Gupta and Maranas, 2000). Recent development of algorithms of this approach has made it possible to solve large-scale linear and mixed-integer linear process planning problems (Clay and Grossmann, 1997). However, the application of recourse is limited since in many cases a suitable measure of compensation of the constraint violation is not available. In these cases, the approach of *chance constraints* can be used, in which a user-defined level of probability of holding the constraints (reliability of being feasible) will be ensured. This is appropriate if constraint violations are unavoidable in certain extreme cases, or if they cause significant costs that cannot be modeled exactly (Kall and Wallace, 1994).

While some uncertain parameters are usually treated as constants during the process operation, there are some time-dependent uncertain parameters which are dependent on the process operation conditions. For instance, the catalyst activity in a catalytic reaction often changes with time. Another example is the uncertainty of the feedstreams coming from the upstream plants, which we will intensively study in this work. A dynamic stochastic optimization problem will in these cases be formulated. For such problems, rather than individual stochastic parameters, continuous stochastic processes should be considered. A special difficulty in solving such problems is to handle the inequality constraints during the time horizon. Arellano-Garcia et al. (1999) consider optimal process operation under time-varying uncertain parameters and use probabilistic (chance) constraints to describe the inequalities. This formulation has an advantage in solving the stochastic programming problem by a simulation framework (Szántai, 1988; Prékopa, 1995). This approach has been recently applied to the design of robust controllers (Schwarm and Nikolaou, 1999; Li et al., 2000a,b). Henrion and Römisch (1999) have studied the stability of optimization approaches under chance contraints if the uncertain variables deviate from normal distributions.

### *Distillation processes under uncertain inflows*

Distillation is one of the most common separation processes which consumes the largest part of energy in the chemical industry. For continuous distillation processes with a fixed feed flow and predefined distillate as well as bottom specifications, a steady-state operating point can be designed based on the knowledge of thermodynamics. During the column operation, this steady state is usually kept by closed control loops which can reject some slight feed disturbances. It is well-known that there is no degree of freedom for carrying out an optimization for such processes. However, there is another usual case in the process industry where the feed of a column is from outflows of several upstream plants. Usually, these streams are first accumulated in a tank (a middle buffer) and then fed to the column, as shown in Figure 1. The streams often change considerably due to the varying operation of the upstream plants. We may have high flow rates of the feed during the main working hours and decreased flow rates dur-

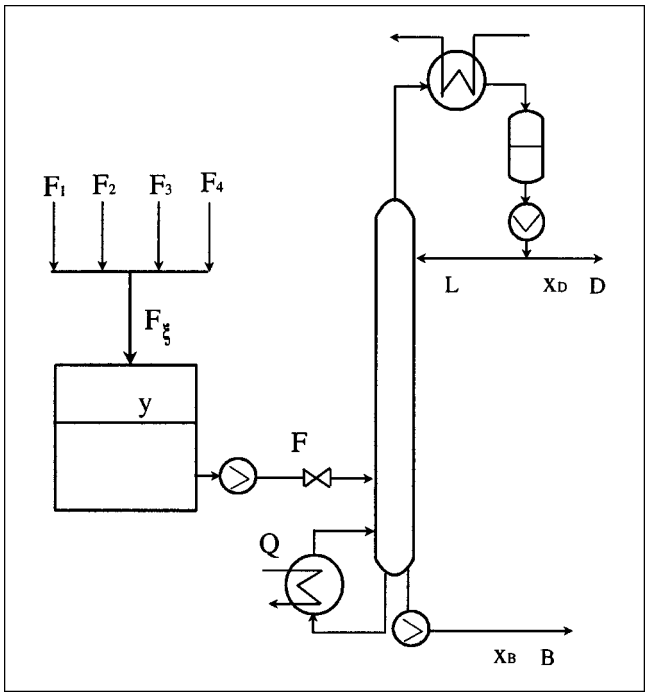


**Figure 1. Distillation process with uncertain feedstreams.**

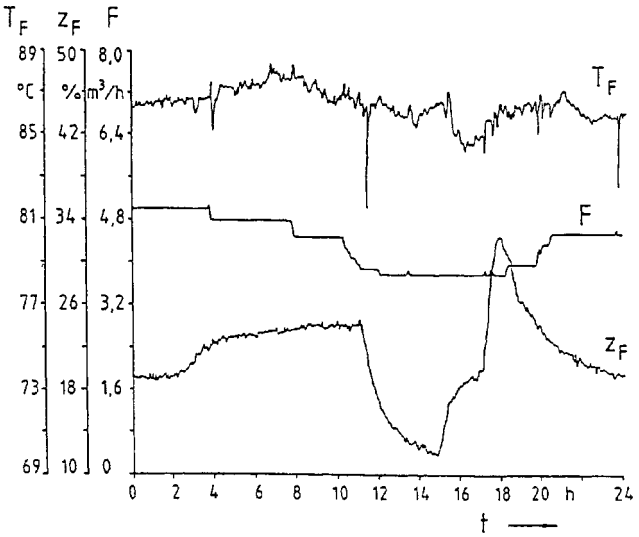


**Figure 2. Measured feed of an industrial methanol-water distillation process.**

ing the night hours or on the weekend. A typical case of such processes is the methanol-water separation plant of large chemical companies. Figure 2 shows the measured profiles of the feed flow rate, composition, and temperature for 24 h from an industrial plant. We only focus here on the impact of the variation of the inflow rate. One consequence resulting from the fluctuating feedstreams is that the tank level $y(t)$ may exceed the upper bound (then a part of the liquid must be pumped out to an extra tank) or fall below the lower bound (then a redundant feedstream must be added to the feed flow). Since large fluctuations of the inflows take place frequently during the operation of such plants and the appearance of these cases (overflow or an empty tank) will lead to considerable extra costs, a careful planning for the operation should be made to prevent it.

Another consequence of a large feed change is that it causes significant variations of the operating point of the downstream column. Due to this large disturbance, the feedback control loops are often not capable of following the required changing operating point because of the strong nonlinearity and the large time delay of the plant. A conservative set point is usually used to guarantee the product quality ($x_D$ and $x_B$) for a higher purity than the required specification. This leads however to more energy consumption than required. The growth of energy requirement for a column operation is very sensitive to the product purity, especially for a high purity distillation.

In this work we propose a novel decomposed optimization strategy to solve this operation problem. Because of the existing feed tank, the system has a degree of freedom to manipulate its outflow rate (the feed flow to the column). First, an optimal planning will be made to ensure the tank level inside the upper and lower bounds (it is not necessary to keep a tank level exactly) by controlling this stream while keeping a flat outflow. The total inflow to the tank is described by a stochastic process. Stochastic optimization under probabilistic constraints is used to develop the outflow rate policy. As a result, the level of the tank is held in the desired range with a predefined probability and meanwhile the tank outflow is as smooth as possible. Thus, the propagation of the large inflow disturbances from the upstream plants to the column will be minimized. Feasibility issues are analyzed and a new method is proposed to ensure a feasible solution of the stochastic optimization problem. Based on the parameters of the stochastic process as well as the plant model, the maximum reachable probability of the constraints can be computed through a run of simulation.

Since the uncertainty is absorbed in the stochastic optimization over the feed tank, the operation of the column is deterministic. The developed outflow from the tank is considered as the feed disturbance to the column. Since it may change considerably, the operating point of the column must also be altered drastically. Instead of using a feedback control system, a deterministic dynamic optimization is used to develop the reflux rate and reboiler duty policies to minimize the operating energy. In effect this is equivalent to holding the product purities as close as possible to their specification under the changing feed rate. The advantage of a nonlinear optimization is that it can directly utilize the rigorous model. Moreover, an optimal policy for the whole horizon can be developed by the dynamic optimization, that is, it has a nature of prediction. The objective function is defined as minimizing the total operating energy during the defined time period. The equality constraints consist of all model equations, while the inequality constraints are the distillate and bottom composition specifications.

The overall operating strategy is optimal in the sense that the objective of optimization is the minimization of the total operating energy. Considering a feed with a fixed composition, a smoother feed flow will demand less operating energy. Thus, the optimality is obtained by the maximum possible smoothness of feed flow to the column. The proposed approach is applied to a pilot distillation column for separating a methanol-water mixture. For the deterministic optimization, a rigorous dynamic column model is used, which is validated by the simulation and experimental results. The developed operating policies are realized on the real plant.

## Stochastic Optimization for Planning the Dynamic Operation

A feedback control loop is used conventionally in process industry to keep the level of the feed tank using the outflow as the manipulated variable. The drawback of this control loop is that it cannot guarantee the upper and lower level bounds and it will propagate the inflow disturbance to the downstream distillation column. In this section we will develop an optimal planning for the operation of the process by applying stochastic optimization to the feed tank. The constraints are the upper and lower bounds restrictions for the tank level during the whole time horizon. To describe the continuous uncertain inflow, this stochastic process is discretized as multiple stochastic variables in fixed time intervals. We assume that they have a multivariate normal distribution with an available mean profile and a covariance matrix in the time horizon. The reason for this assumption is that the total inflow to the feed tank is the sum of several independent streams from the upstream plants. According to the central limit theorem (Loeve, 1963), if a random variable

is generated as the sum of effects of many independent random parameters, the distribution of the variable approaches a normal distribution, regardless of the distribution of each individual parameter. An example in Papoulis (1965) illustrates a surprisingly good approximation of a normal distribution by the sum of three uniformly distributed parameters (thus, each of those has a distribution very different from Gaussian). The probability density function of a multivariate normal distribution is described by

$$\varphi_N(\boldsymbol{F}_\xi) = \frac{1}{|\Sigma|^{1/2}(2\pi)^{N/2}} e^{-\frac{1}{2}(\boldsymbol{F}_\xi - \boldsymbol{u})^T \Sigma^{-1}(\boldsymbol{F}_\xi - \boldsymbol{u})} \tag{1}$$

where $\boldsymbol{F}_\xi = [F_\xi(1), \ldots, F_\xi(N)]^T$ is the vector composed of the uncertain inflow rate in each individual time interval. $\boldsymbol{\mu}$ and $\boldsymbol{\Sigma}$ are known mean values and the covariance matrices of these stochastic variables, which have the following form

$$\boldsymbol{\mu} = \begin{bmatrix} \mu_1 \\ \mu_2 \\ \cdots \\ \mu_N \end{bmatrix} \quad \boldsymbol{\Sigma} = \begin{bmatrix} \sigma_1^2 & \sigma_1\sigma_2 r_{12} & \cdots & \sigma_1\sigma_N r_{1N} \\ \sigma_1\sigma_2 r_{12} & \sigma_2^2 & \cdots & \sigma_2\sigma_N r_{2N} \\ \cdots & \cdots & \cdots & \cdots \\ \sigma_1\sigma_N r_{1N} & \sigma_2\sigma_N r_{2N} & \cdots & \sigma_N^2 \end{bmatrix} \tag{2}$$

where $\sigma_i$ is the standard deviation of each individual stochastic variable and $r_{ij} \in [-1, 1]$ the correlation coefficients between $F_\xi(i)$ and $F_\xi(j)$. It should be noted that often a strong correlation between the uncertain variables exists for time-varying stochastic processes. A positive correlation ($r_{ij} > 0$) means, if a variable is larger (smaller) than the mean value in a time interval, the variable is likely to be larger (smaller) than the mean value in the next time interval as well. The reverse is true if the sign of the correlation coefficient is negative. The existence of a correlation will lead to larger output deviations from the expected values and thus causes a higher probability of violating the output constraints.

Figure 3 shows the sampled profiles of the inflow rate where $\sigma_i = 0.05$ ($i = 1, \cdots, N$) and $r_{ij} = r_{ji} = 1 - 0.05(j - i)$ ($i = 1, \cdots N$, $j = i + 1, \cdots, N$). With this distribution of the inflow rate, it is not possible to decide the outflow of the tank to guarantee the level absolutely in the specified region. Therefore, the following stochastic optimization problem is defined, which consists of a probabilistic (chance) constraint. This means that inequality constraints are to be held with a predefined probability level

$$\begin{aligned} &\min \sum_{i=0}^{N-1} \left[F(i) - F_0\right]^2 \\ &\text{s.t. } y(i+1) = a\,y(i) + b\left[F_\xi(i) - F(i)\right] \quad y(0) = y_0 \\ &P\{y_{\min} \le y(i) \le y_{\max}, \quad i = 1, \cdots, N\} \ge p \\ &F_{\min} \le F(i) \le F_{\max} \end{aligned} \tag{3}$$

where $F_0$ is the specified value of the total flow rate to the column, according to the column design. $a$ and $b$ are constants related to the tank area and the length of the time interval. $y_0$ is the initial tank level. Due to the existence of the stochastic variables and the chance constraint, this is a stochastic optimization problem. This problem can also be considered as a predictive control system under uncertainty. In effect, Eq. 3 can be regarded as an optimal control problem, where $y(t)$ is the output and $F(i)$ is the input variable, and $F_\xi(i)$ is the disturbance, if a moving horizon is introduced. In Eq. 3 a *joint* change constraint is used, which concerns the joint probability of satisfying all of the inequalities in the whole horizon. Another form of chance constraint is a *single* probabilistic constraint which concerns the individual time point

$$P\{y_{\min} \le y(i) \le y_{\max}\} \ge p \quad i = 1, \cdots, N \tag{4}$$

Obviously, a joint constraint is more stringent than all single chance constraints, but leads to a more difficult problem. We propose to use the method of Szántai (1988) and Prékopa (1995) to solve the problem with joint chance constraints. The idea of the solution method is to relax the stochastic problem to a nonlinear programming problem, so that it can be solved with a standard NLP algorithm such as successive quadratic programming (SQP). In the case of a linear problem with a *joint* chance constraint, the relaxed problem is convex (Kall and Wallace, 1994). The probabilities and gradients of the constraints, composed of stochastic variables with multivariate normal distribution, can be computed using an efficient simulation approach (Prékopa, 1995).

Figure 4 shows the optimal outflow policies with specified probabilities (two scenarios) under the uncertain inflow disturbance shown in Figure 3. 16 time intervals inside the time horizon are chosen as the dimension of the problem. The model parameters in Eq. 3 are set to $a = b = 1$. It can be seen that the optimal outflow policies are much more smooth than the inflow profiles shown in Figure 3. Moreover, the outflow will be inclined to the inflow if the required probability to hold the level restriction is increased. Figures 5 and 6 show the level trajectories resulted from the optimal outflow policies with 10 samples of the inflow rate $\boldsymbol{F}_\xi$. Comparing Figure 5 with Figure 6, it can be seen that, by implementing the outflow derived with the constraint $P \ge 0.9$, it is more likely to violate the level restrictions than that with the constraint $P \ge 0.95$.

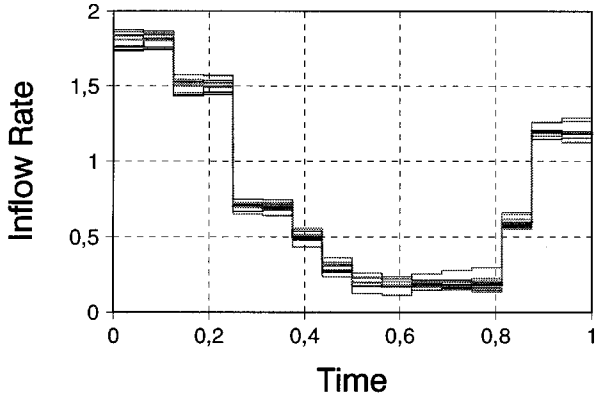


**Figure 3. Inflow rate through 10 samples.**

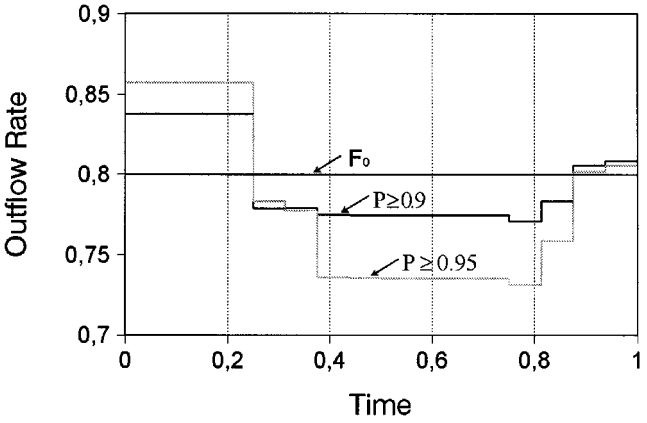


**Figure 4. Optimal outflow rate with different chance constraints.**

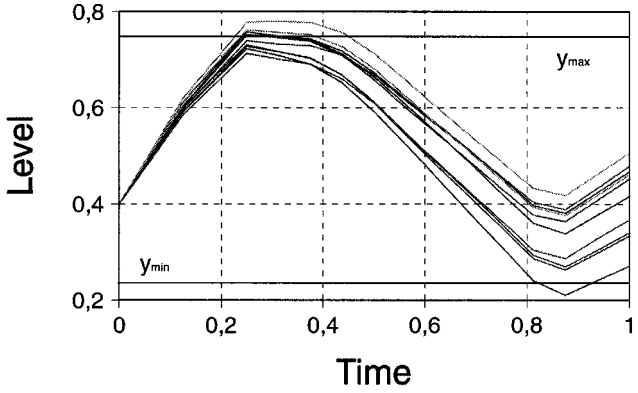


**Figure 6. Tank level realized by 10 samples with the outflow for $P \geq 0.9$.**

## Feasibility Analysis of the Stochastic Optimization Problem

The approach described above takes into account the stochastic information on the inflow streams in a future time horizon. The feasible set of the problem is dependent on the prescribed probability level $p$. Increasing the probability level $p$ in Eq. 3 will decrease the feasible set. The feasible set becomes empty starting from a value $\hat{p}$. A user of the above solution method may unintentionally choose a value of $p$ larger than $\hat{p}$. Then, SQP will not find a solution to the problem. Therefore, it is important to analyze feasibility issues and thus to ensure a solution. Previous studies (Prékopa, 1995) suggest a probability maximization step to obtain the maximum probability value $\hat{p}$. In this work, we propose a new solution method that takes only one run of simulation to compute this value.

Consider the output (level) at each time point as a variable determined by the control (outflow) and disturbance (inflow) trajectories, then the feasibility of the probabilistic constraint in Eq. 3 means that the variables can be held in an $N$-dimensional hypercube with a specified probability level. Although the problem can be solved, there may be no feasible solution at all in some cases, which implies that the chance constraints cannot be satisfied by any possible input trajectories. Thus, we have to determine whether the defined problem has a feasible solution or not. This is especially important when the solution of the problem is carried out online.

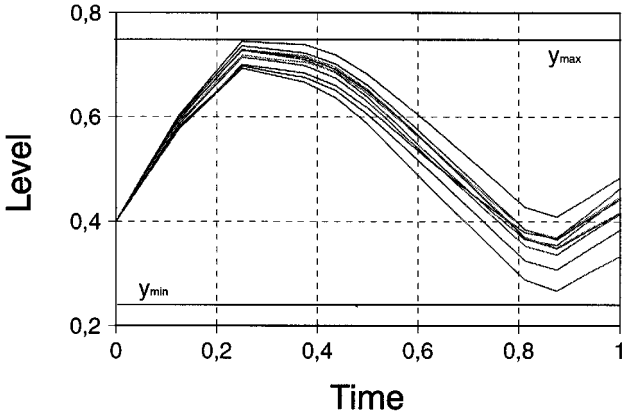


**Figure 5. Tank level realized by 10 samples with the outflow for $P \geq 0.95$.**

### *One-step prediction*

Instead of the tank model in Eq. 3, we now consider a general linear stable plant

$$y(i+1) = ay(i) + bu(i) + c\xi(i) \tag{5}$$

where $a$, $b$, and $c$ are known model parameters, and $y$ and $u$ are output and input variables, respectively. $\xi$ is the stochastic disturbance variable described by Eqs. 1 and 2. Let us first limit the predicted horizon to *one* future point. The constraint in Eq. 3 is reduced to

$$\mathrm{P}\{y_{\min} \leq y(1) \leq y_{\max}\} \geq p \tag{6}$$

From Eq. 5, we can derive the mean and the standard deviation of $y(1)$

$$\mu_{y(1)} = ay(0) + bu(0) + c\mu_1 \tag{7}$$

$$\sigma_{y(1)} = |c|\sigma_1 \tag{8}$$

It is interesting to note that the input value can change the mean value of the future output, but has no effect on its variance. Since, for a normally distributed disturbance, the output of a linear system is also normally distributed, the chance constraint (Eq. 6) is equivalent to

$$\Phi_1\left(\frac{y_{\max} - \mu_{y(1)}}{\sigma_{y(1)}}\right) - \Phi_1\left(\frac{y_{\min} - \mu_{y(1)}}{\sigma_{y(1)}}\right) \geq p \tag{9}$$

where $\Phi_1$ is the one-dimensional (1-D) standard normal probability distribution function. Figure 7 depicts the relations between the parameters in Eq. 9. The probability will be different with different output variances resulted from Eq. 8, as shown in Figure 7 with $\sigma_y' < \sigma_y'' < \sigma_y'''$. With $\sigma_y'$ we have the freedom to move $\mu_{y(1)}$ with $u(0)$, since the feasible region

is large enough. If the output standard deviation is as large as $\sigma_y''$, there will be no freedom, that is, $u(0)$ must have the value such that $\mu_{y(1)}$ lies at the middle of $[y_{\min}, y_{\max}]$. It implies that the feasible region is reduced to one point. If $\sigma_{y(1)}$ is larger than $\sigma_y''$ (like $\sigma_y'''$ as shown in Figure 7), the problem will have no feasible solution. Therefore, $\sigma_1$ decides the feasibility of the system, if the input is unconstrained. According to Eq. (9), to make sure the problem has a solution there must be

$$\sigma_1 \le \frac{y_{\max} - y_{\min}}{2|c|\Phi_1^{-1}\left(\frac{p+1}{2}\right)} \tag{10}$$

where $\Phi_1^{-1}$ is the inverse function of $\Phi_1$. From this representation, it can be concluded that we can relax an infeasible problem of this kind by lowering the probability level $p$ or by enlarging the specified output region $[y_{\min}, y_{\max}]$.

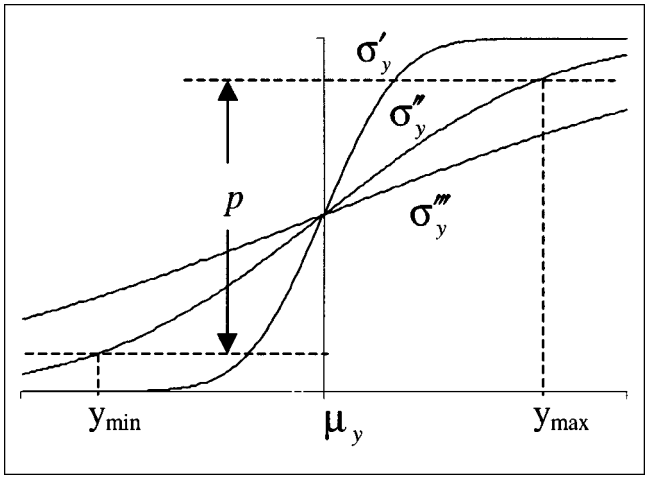


**Figure 7. Probability in respect to the output variable.**

### *N-step prediction*

For a horizon with $N$ predictive points, from Eq. 5, the output on each time point can be described as

$$y(i) = a^i y(0) + b\sum_{l=1}^{i} a^{l-1}u(i-l) + c\sum_{l=1}^{i} a^{l-1}\xi(i-l) \qquad i = 1, \cdots, N \tag{11}$$

From Eq. 2, the mean of the output is then

$$\mu_{y(i)} = a^i y(0) + b\sum_{l=1}^{i} a^{l-1}u(i-l) + c\sum_{l=1}^{i} a^{l-1}\mu_{i-l+1} \tag{12}$$

The covariance of the output between point $i$ and $j$ ($j \ge i$, $i = 1, \cdots, N$) can be computed by

$$\begin{aligned} R_y(i,j) &= \mathrm{E}\{[y(i) - \mu_{y(i)}][y(j) - \mu_{y(j)}]\} \\ &= c^2\mathrm{E}\left\{\left[\sum_{l=1}^{i} a^{l-1}[\xi(i-l) - \mu_{i-l+1}]\right] \times \left[\sum_{m=1}^{j} a^{m-1}[\xi(j-m) - \mu_{j-m+1}]\right]\right\} \\ &= c^2\sum_{l=1}^{i}\sum_{m=1}^{j} a^{i+j-l-m}\sigma_l\sigma_m r_{l,m} \end{aligned} \tag{13}$$

which will contribute to the correlation of these two points. The variance of the output at point $i$ is then

$$\sigma_{y(i)}^2 = R_y(i,i) = c^2\sum_{l=1}^{i}\sum_{m=1}^{i} a^{2i-l-m}\sigma_l\sigma_m r_{l,m} \tag{14}$$

which is a part of the covariance (Eq. 13). Again, it can be seen from Eq. 12 and Eq. 14 that the input can only affect the means of the outputs, which horizontally shifts an individual probability profile (see Figure 7). From Eqs. 13 and 14 the output covariance (and variance) is determined by the covariances of the disturbance at different time points, as well as the model parameters ($a$ and $c$). The covariance will affect the shape of the probability curve. Therefore, for a problem with $N$ predictive points, the feasibility depends on the output covariance matrix if the input is unconstrained (or the allowable region of inputs is large enough). Moreover, due to the high-order exponential terms, both the means and the covariances of the outputs are highly sensitive to the values of the model parameter $a$.

### *Under single chance constraints*

If we consider the single chance constraints (Eq. 4), the relation (Eq. 9) can be used here for the inequality constraint of each individual output point, since the output of a linear system disturbed by a normally distributed sequence is also normally distributed. This means

$$\Phi_1\left(\frac{y_{\max} - \mu_{y(i)}}{\sigma_{y(i)}}\right) - \Phi_1\left(\frac{y_{\min} - \mu_{y(i)}}{\sigma_{y(i)}}\right) \ge p \quad i = 1, \cdots, N \tag{15}$$

where $\mu_{y(i)}$, $\sigma_{y(i)}$ are computed from Eqs. 12 and 14, respectively. Manipulating $u(i)$ such that $\mu_{y(i)}$ is at the middle of $[y_{\min}, y_{\max}]$, the reachable maximum value of the individual probability will be

$$\mathrm{P}_{\max}(i) = 2\Phi_1\left(\frac{y_{\max} - y_{\min}}{2\sigma_{y(i)}}\right) - 1 \quad i = 1, \cdots, N \tag{16}$$

By comparing $\mathrm{P}_{\max}(i)$ with $p$, we can know whether the problem is feasible or not. The required input values $u(i)$ corresponding to this achievable probability can be calculated through Eq. 12.

### *Under a joint chance constraint*

For the joint chance constraint in Eq. 3 with $N$ output points, it is impossible to derive an explicit probability representation like Eqs. 15 and 16. However, we know that large absolute values of the elements in the output covariance matrix may cause an infeasible problem. From Eqs. 13 and 14,

we have the following relations between the output covariance of a point and that of the point before

$$R_y(i,i+1) = c^2\left(a\sigma_{y(i)}^2 + \sum_{l=1}^{i} a^{i-l}\sigma_l\sigma_{i+1}r_{l,i+1}\right) \quad (17)$$

$$\sigma_{y(i+1)}^2 = c^2\left(a^2\sigma_{y(i)}^2 + \sum_{l=1}^{i+1} a^{i+1-l}\sigma_l\sigma_{i+1}r_{l,i+1} + \sum_{m=1}^{i} a^{i+1-m}\sigma_m\sigma_{i+1}r_{i+1,m}\right) \quad (18)$$

from which one can observe the change of the values of the output covariance (variance) from one time point to the next. In addition to the variance of the disturbance at each individual point, the correlation between the points of the stochastic sequence has an effect on the increase of the variance of the next output. For small element values in the output covariance matrix, it is desired to have small correlation coefficients $r_{i,j}$ in the disturbance covariance matrix. As for the model parameters, it is shown from Eq. 17 and Eq. 18 that $|c| < 1$ and $|a| < 1$ is favorable for the feasibility of the system. Another factor affecting the value of the covariance (variance) is the length of the horizon. For example, if $a = 1$, $\sigma_i = \sigma$, $r_{i,j} = 0$, $(i \neq j,\ i,j = 1,\ \cdots,\ N)$, the variance of the output at point $N$ will be

$$\sigma_{y(N)}^2 = c^2\sigma^2 N \quad (19)$$

Compared with Eq. 11, the variance of the output at point $N$ is $N$ times higher than the value of that at the first point. In this case, a larger $N$ will more possibly lead to an infeasible problem.

Although we have no explicit function for calculating the joint multivariate probability, its maximal achievable value can be computed based on the theorem given in the Appendix. In the Appendix we prove that the joint probability has the maximum value if the mean values of the output vector are at the middle of $[y_{\min},\ y_{\max}]$ for $i = 1,\ \cdots,\ N$, namely

$$\mu_{y(i)} = \frac{y_{\min} + y_{\max}}{2} \quad i = 1,\ \cdots,\ N \quad (20)$$

Replacing $\mu_{y(i)}$ in Eq. 12 with $\mu_{y(i)}$ in Eq. 20, the corresponding input vector can be calculated by

$$u(i-1) = \frac{1}{b}\mu_{y(i)} - \frac{a^i}{b}y(0) - \frac{c}{b}\sum_{l=1}^{i} a^{l-1}\mu_{i-l+1} - \sum_{l=2}^{i} a^{l-1}u(i-l) \quad i = 1,\ \cdots,\ N \quad (21)$$

With this control vector, the maximal achievable joint probability can be computed through one run of simulation by the method described earlier. Table 1 shows the results of maximal achievable probabilities to hold the lower and upper level restrictions in problem 3 with $a = b = 1$, $y(0) = 4$, and $y_{\min} = 2.5$, $y_{\max} = 7.5$ (see Figures 5 and 6). The parameters describing the multivariate normal distribution are set with $\sigma_i = \sigma$ $(i = 1,\ \cdots,\ N)$ and $r_{ij} = 1 - \theta(j-i)$ $(i = 1,\ \cdots\ N,\ j = i+1,\ \cdots,\ N)$. It can be seen that, as the value of the standard deviation of the disturbance variables increases, the maximal reachable probability will decrease. A stronger correlation ($\theta = 0.05$) between the variables more likely leads to violations of the constraints.

**Table 1. Maximal Achievable Probability of Holding Constraints**

| | $\sigma = 0.05$ | $\sigma = 0.1$ | $\sigma = 0.2$ |
|---|---|---|---|
| $\theta = 0.05$ | $p = 0.999$ | $p = 0.965$ | $p = 0.805$ |
| $\theta = 0.1$ | $p = 1.0$ | $p = 0.986$ | $p = 0.854$ |

## Deterministic Optimization of the Column Operation

The downstream column will be operated with the optimal feed policy developed by the approach described in the second section. The question now is how to operate the column to keep the distillate and bottom composition specification under this feed profile. This principally leads to a control problem. Two control loops are designed to carry out this task conventionally to manipulate the reflux rate and the reboiler duty. However, due to the changing feedstream, the operating point should also be changed frequently. Since distillation is a strong nonlinear process, the conventional control loop cannot follow the desired changing operating point. Thus, a conservative set point value higher than the purity specifications is usually chosen. However, since the energy requirement for a column operation increases sensitively to the product purity, especially for a high purity distillation, a conservative operation leads to much more energy consumption than required. Therefore, we propose to use a nonlinear dynamic optimization to solve the column operation problem. It should be noted that this is a deterministic optimization problem, since the uncertainty in the feedstream variability is absorbed in solving the stochastic problem. A dynamic optimization has three well-known advantages over the conventional feedback control: (i) it employs the nonlinear rigorous model; (ii) it concerns a future time horizon; and (iii) it can keep inequality constraints.

### *Problem formulation*

The objective function is defined as minimization of the total energy in the considered time horizon $[t_0,\ t_f]$, by developing the optimal reflux rate and reboiler duty policies. The equality constraints are the model equations of the distillation column. For the purpose of operation study, it is necessary to select a more accurate model. We here use a rigorous dynamic model shown in Figure 8, where $i = 1,\ \cdots,\ NK$ and $j = 1,\ \cdots,\ NST$ are the indices of components and trays (from the condenser to the reboiler), respectively. The state variables on each tray are the vapor and liquid compositions ($y_{i,j}$, $x_{i,j}$), vapor and liquid flow rate ($V_j$, $L_j$), the liquid holdup $HU_j$, temperature $T_j$, and pressure $P_j$. The model equations include component and energy balances, vapor-liquid equilibrium (VLE) equations, a liquid holdup equation, as well as a pressure drop equation (hydraulics) for each tray of the col-

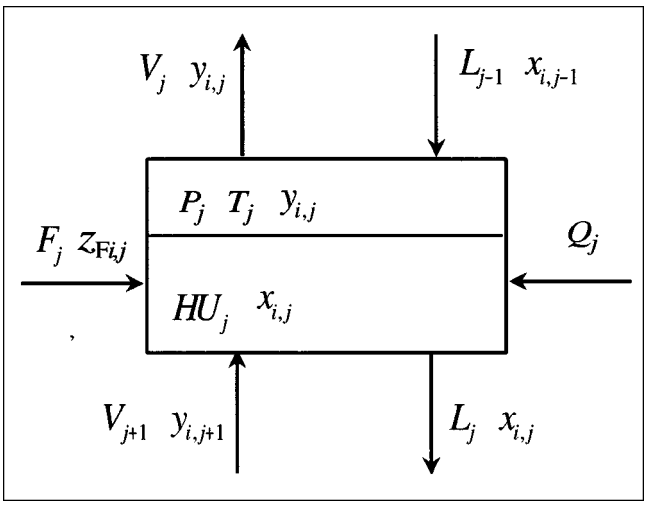


**Figure 8. Model of a general tray in the column.**

umn. Moreover, models like Wilson, NRTL, and so on are used for the VLE calculation. Murphree tray efficiency is introduced to describe the nonequilibrium behavior. This is a parameter that can be verified by comparing the simulation results with the operating data. Rigorous computation in the model also includes the calculation of the component pressure and the vapor, as well as the liquid enthalpy. The inclusion of the tray hydraulics is necessary to describe the dynamic behavior for the dynamic optimization. These lead to a nonlinear index-one DAE system. The inequality constraints consist of the distillate and bottom product specifications, as well as the physical limitations of the reflux rate and the reboiler duty. Thus, a complicated dynamic optimization problem is formulated, which has the following objective function

$$\min \int_{t_0}^{t_f} Q(t)\,dt \tag{22}$$

In addition, auxiliary equations are required to describe the thermodynamic and physical relations in order to compute unknowns which are functions of the state variables. The total number of variables of the problem is $(2NC+5)NST$. The time horizon $[t_0, t_f]$ should be long enough to be able to reflect the nonlinear dynamic behavior of the plant. Thus, we transform the conventional control problem to an optimization problem. It should be noted that it is not equivalent to an optimal control problem for the column, which usually uses a quadratic function as the objective function to minimize the deviation of the distillation and bottom functions from their specifications.

### *Solution approach*

Although there have been approaches to solve large-scale dynamic optimization problems, few reports on the solution of such complex problems formulated together with the auxiliary equations have been, to our knowledge, found in literature. Li (1998) proposes a sequential approach to solve such problems. Both the state and the control variables are discretized on finite elements. In each element the state variables are approximated with orthogonal polynomials, while the piecewise constant form is used for the controls. The approach consists of an optimization layer, where the controls in each element will be solved by SQP, and a simulation layer, where the total equation system is integrated and the sensitivities required by SQP are computed. The approach is efficient, since all equations (that may be very complicated) are not included in SQP. It has been successfully applied to several real processes (Li et al., 1998; Wozny and Li, 2000; W et al., 2000).

Until now, we have defined two (decomposed) optimization problems for such processes as shown in Figure 1: a stochastic optimization over the feed tank with the objective function given in Eq. 3 and a deterministic optimization over the downstream column with the objective function (Eq. 22). By solving the former problem, a smooth outflow from the tank will be determined, while, with this flow as the feed to the column, the policies of reflux and reboiler duty of the column will be developed by solving the latter problem. Attention should be paid to the optimality of the overall strategy.

Our aim of optimization is to minimize the total operating energy under the uncertain streams to the feed tank. Meanwhile the distillate and the bottom purity specification must be satisfied. Considering the process shown in Figure 1, the overall operating energy consumed by the column will be minimal if the compositions of the distillate and the bottom flow are well kept at the values of their purity specification (purer than specified is allowable but more energy will be needed). To achieve this, proper reflux and reboiler duty policies will be developed, which is the task of the deterministic optimization. However, due to the oscillation of the feedstream of the column, it is impossible to keep the compositions right at their specifications, that is, higher than those values will be realized (lower than specification is not allowed). Therefore, the overall minimum operating energy is reached if the feed flow rate of the column is kept as smooth as possible, which is the task of the stochastic optimization.

## Application to a Pilot Distillation Column

Although many theoretical investigations on dynamic optimization have been made, very few studies have been done on their verification on real plants. In this section, the optimization strategy proposed is applied to a pilot distillation column in our lab. The flow sheet of the plant is similar to Figure 1. The column has a diameter of 100 mm and 20 bubble-cap trays with a central downcomer. Isolation coat has been mounted to prevent the heat loss from the column wall. The boilup is provided by an electrical reboiler with a maximum duty of 30 kW. The condensation is carried out by a total condenser with cooling water. The plant is equipped with temperature, pressure, level, and flow rate measurements and electrical valves for flow control. All input/output signals are treated by a process control system. Several control loops have been configured and implemented on the plant. The control system is connected to the local area network to manage experimental data. The composition of the feedstream, distillate and bottom product is measured off-line with a gas chromatograph.

### *Model validation*

The column is to be used to separate a methanol-water mixture to high purity products. The column is operated at the atmospheric pressure. We use the column model described in the last section. The Wilson model is used for computing the VLE and its parameters are from Gmehling et al. (1977). Parameters of the pure components are from Reid et al. (1987). The parameters for the tray holdup and the pressure drop calculated by the gas and liquid fluid dynamics are based on the tray geometric sizes. Several parameters (coefficients) in the model are strongly dependent on the column structure and the operating point and thus should be matched to the experimental results. We consider the tray efficiency in the rectifying section $\eta_R$ and stripping section $\eta_S$ of the column, the weir constant $C_W$ for the holdup calculation, the friction factor $\zeta_W$ for the calculation of the dry pressure loss, as well as the total heat loss $Q_V$ from the column. The result of $Q_V$ is important for the implementation of the computed reboiler duty values $Q_{\text{eff}}$ on the real plant.

To accomplish the above verifications, 10 steady-state operating points have been gained through experiment. The measured data (temperature, pressure as well as pressure drop, flow rates, compositions, and reboiler duty) are compared with the simulation results by adjusting the parameters with trial-and-error. Moreover, the measured data of the dry pressure drop of the rectifying section and the total pressure drop of the stripping section during the startup phase were also used for estimating the parameters $\zeta_W$ and $C_W$. To verify these values, step changes of feed rate, reflux rate, and reboiler duty were given from a steady-state operating point during an experiment. Figure 9 shows the temperature responses along the column, where the black lines with noises are the measured curves and the gray lines are the simulated results. It can be seen that a very good agreement has been received for the top and bottom temperature. The temperature on tray 17 and 18, which are the two most sensitive trays in the column, has a 2–3°C difference between the measured and computed results. The reason for this is the existing slight disturbances from the atmospheric pressure and temperature during the experiment which led to the oscillation of the column pressure and heat loss from the column.

The fact that both the measured and simulated curves have the same tendency demonstrates that the inclusion of the hydraulic computation leads to a successful description of the dynamic behavior for the column operation. It can be noted that the temperature on the trays in the rectifying section is not sensitive to the step changes, especially for the top of the column. However, the temperature in the stripping section has a significant sensitivity. This phenomenon can be identified from the form of the x-y-diagram of the methanol-water mixture (Gmehling et al., 1977).

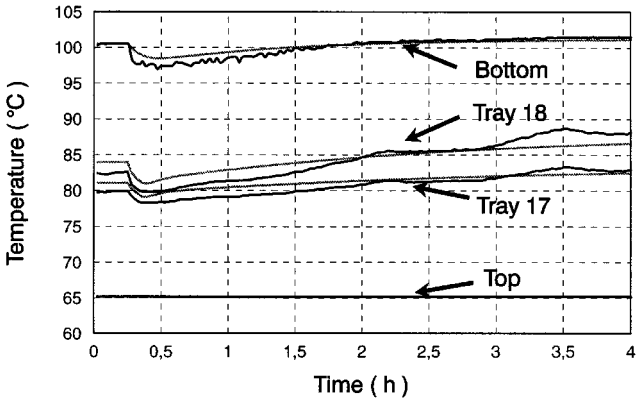


**Figure 9. Simulated and measured temperature.**

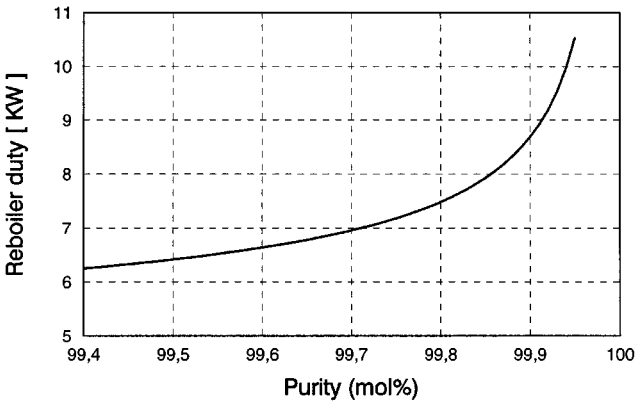


**Figure 10. Energy requirement of the pilot column operation with different purity specifications.**

### *Optimization results*

The deterministic optimization approach is applied to the verified column model, with the feed flow rate trajectory given by the stochastic optimization over the tank. We consider 5 h as the time horizon with an initial steady state at $F = 20$ L/h, $z_F = 30$ mol % with the reflux rate and reboiler duty $L = 14.7$ L/h, $Q_{\text{eff}} = 6.414$ kW, respectively. Figure 10 shows the reboiler duty of the column due to different distillate and bottom purity specifications in steady-state operation. It indicates that the energy requirement increases exponentially with an increasing purity. For the dynamic operation, we assume that both the distillate and the bottom purity should be higher than 99.5 mol %, which are the two path inequality constraints for the dynamic optimization. The two control variables (reflux rate and reboiler duty) are discretized as piecewise constants in 20 time intervals with a length of 0.25 h for each interval. For starting the computation the guess policies of the two variables are given as constants during the time horizon.

To analyze the energy requirement under different feed flow rate, a smooth case and a drastically changing case are considered, as shown in Figure 11. The total amount of the feed to be separated in the time horizon are the same in the two cases. This amount is also equivalent to the total amount of feed at the steady-state. Thus, if the purity constraints are exactly satisfied ($x_D = x_B = 99.5$ mol %) during the horizon, the theoretical energy consumption in the two cases should have the same value as required by the steady-state operation. According to the optimization results, however, the total energy consumption in case 1 is $E_1 = 115.454$ MJ and in case 2 it is $E_2 = 118.739$ MJ. This means that the purity constraints can be almost exactly satisfied during the time horizon if the feed rate trajectory is relatively smooth like Case 1.

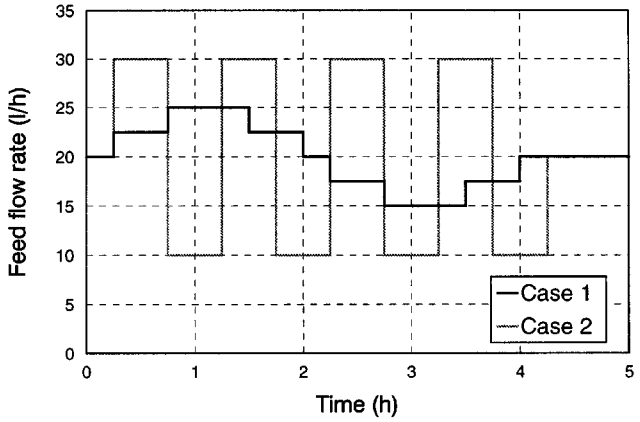


**Figure 11. Feed flow rate to the distillation column.**

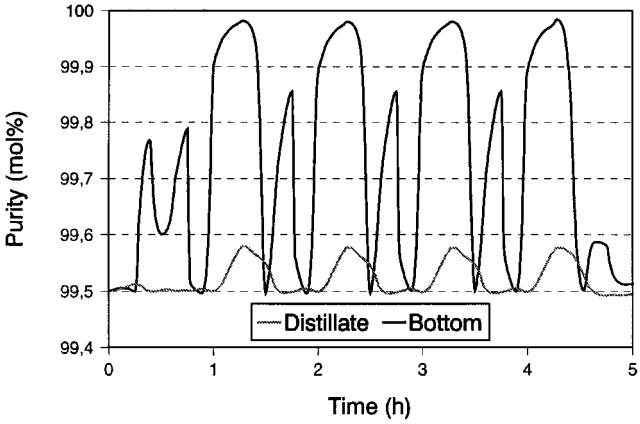


**Figure 13. Optimal purity (Case 2).**

In the second case a higher purity than required has to be realized to ensure the constraints to be held under the drastically changing feedstream. Figures 12 and 13 show the optimal distillate and bottom purity trajectories of the two cases. Both products are purer than, but tend to their specifications, which demonstrate a high quality of the optimization approach. Considering the complexity of the plant (nonlinear, time delay, and interaction between the variables), it is impossible to achieve such a performance by using a conventional feedback control system.

The distillate purity profiles are not sensitive to the changes of the feedstream and thus there is almost $x_D = 99.5$ mol %. Obvious differences of the bottom purity between the two cases can be observed. These case studies demonstrate the conclusion that, for the optimal operation of such processes as shown in Figure 1, the outflow of the feed tank should be kept as smooth as possible to reduce the energy consumption, as long as probabilistic level constraints are satisfied. This means that the optimality of the overall strategy is obtained by implementing the smooth flow to the column developed in the stochastic optimization.

Figures 14 and 15 show the optimal operating policies for the two feed cases. It is interesting to note that in both cases both the reflux rate and the reboiler duty have the same tendency as the column feed flow. This implies that a feed forward control may improve the operating quality of this column. Another remark from these results is that reflux rate takes part in the campaign against the feed disturbances, although the distillate purity constraint is constantly satisfied. This shows another advantage of nonlinear optimization that concerns the whole multivariable system over conventional control loops that concern only the individual input and output variables.

### *Implementation on the real plant*

An experimental implementation of the optimization results was done on the pilot plant by considering a feed flow trajectory to the column. The column was initially operated at a steady-state point with $F = 15$ L/h, $z_F = 30$ mol % fed to the 14th tray from the top of the column. Before conducting the experimental run, the optimal reflux flow and reboiler policies were computed by the optimization approach. Then the profiles of the feed flow, the reflux flow, and the reboiler duty were realized at the column, as shown in Figure 16. It should be noted that the lower bound of the reflux $L_{\min} = 9.6$ L/h was set in the computation due to the minimal liquid load in the column.

Figure 17 shows the measured temperature profiles of the condenser and of every two trays in the column and of the reboiler. As the feed flow was increased during the first pe-

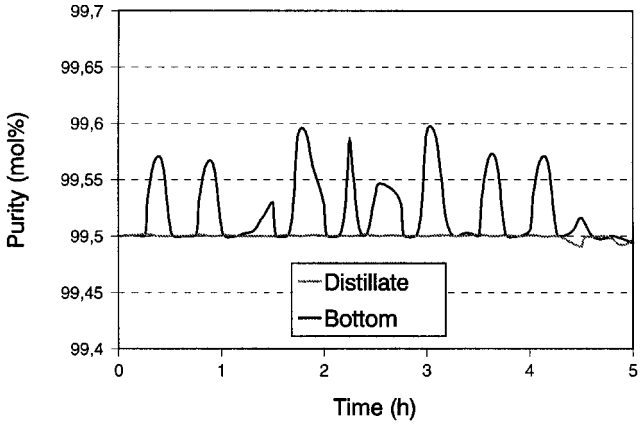


**Figure 12. Optimal purity (Case 1).**

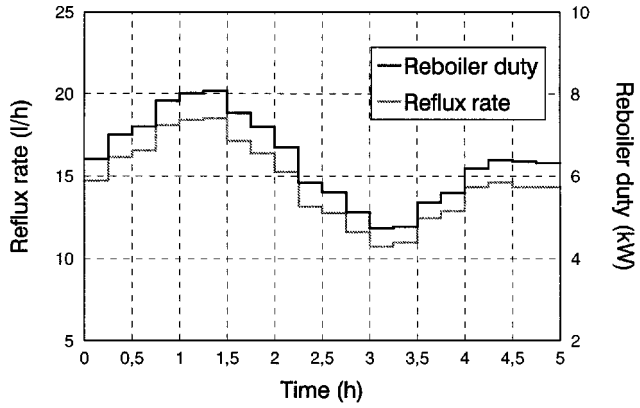


**Figure 14. Optimal policy for Case 1.**

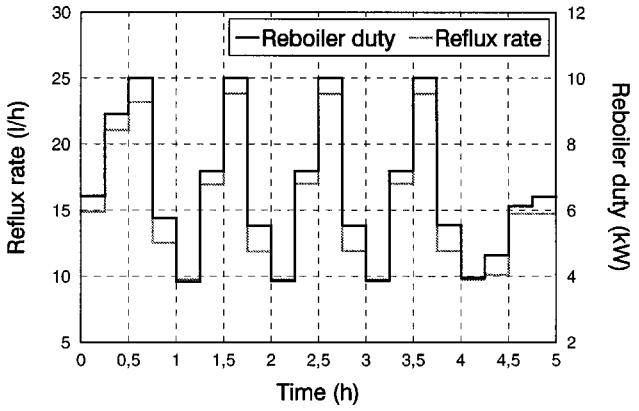


**Figure 15. Optimal policy for Case 2.**

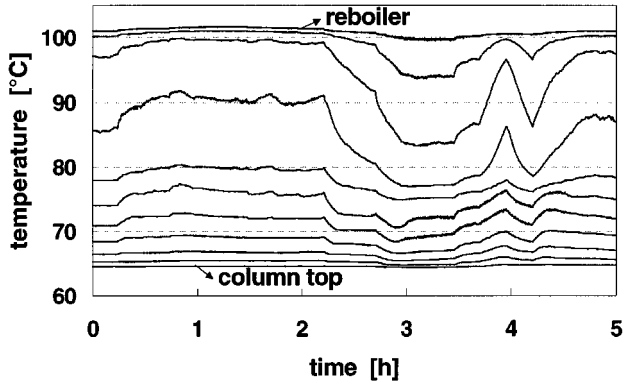


**Figure 17. Measured temperature trajectories in the condenser of every two trays in the column and in the reboiler by the optimal control policy.**

riod, both the reflux flow and the reboiler duty, according to the optimization results, should be raised to compensate the feed increase. However, this led to the increase of the pressure drop in both of the stripping and rectifying section, as shown in Figure 18. This larger pressure drop caused a higher operating pressure on the trays and the bottom of the column and thus led to the increase of their temperature during the first 2 h (the pressure of the column top was the atmospheric pressure that was 1.03 bar during the experiment). At a higher bottom pressure, a slightly higher equilibrium temperature was required for keeping the bottom product purity, which can be seen in Figure 17.

During the second time period, as the feed flow was decreased, both the reflux and the reboiler duty were reduced. This caused the decrease of the column pressure drop, particularly in the rectifying section. The pressure drop was only about 1 mbar per tray in the rectifying section at the minimum point. It implies that the tray efficiency in the section was much smaller during this period than that in the period before, reflecting the lower bound of the liquid load of the column. It is interesting to note that the larger temperature differences of the trays in the stripping section, as shown in Figure 17, indicate that this section took the most separation task during this period. Moreover, due to the smaller pressure drop, the operating pressure of the bottom was reduced and thus the bottom temperature was also decreased. As the feed and the operating policy reverted to their initial values at the end, the column operation tended to return to the initial steady state.

To obtain a quantitative qualification on the energy saving from the optimization results, a comparative experiment was done, during which two well-tuned PID-controllers were used to control the top and bottom temperature with fixed set points. The same feed profile shown in Figure 16 was fed to the column. Figure 19 shows the trajectories of the feed and the two control variables, and Figure 20 showed the measured temperature trajectories resulting from the controllers. Although the temperatures can be well kept at their set points, the operation is not optimal. The product purity will be either lower than the specification (constraint violation during the first period) or higher than the specification (more energy consumption during the second period). The total energy consumed during the time period was 101.083 MJ by the PID controllers, while it was 98.858 MJ by the optimal policies shown in Figure 16.

The results of the plant study indicate that the tray efficiency is sensitive to the feed flow rate. Thus, a proper correlation or an online estimation of tray efficiency is necessary in such cases to enhance model accuracy. This problem is studied by Wendt et al. (2001a). Another result from the ex-

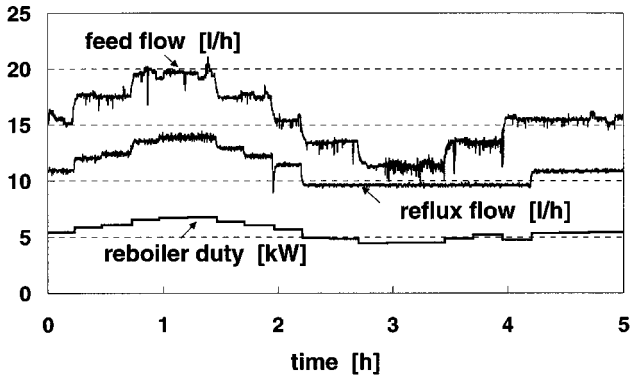


**Figure 16. Implemented feed flow, reflux flow, and reboiler duty.**

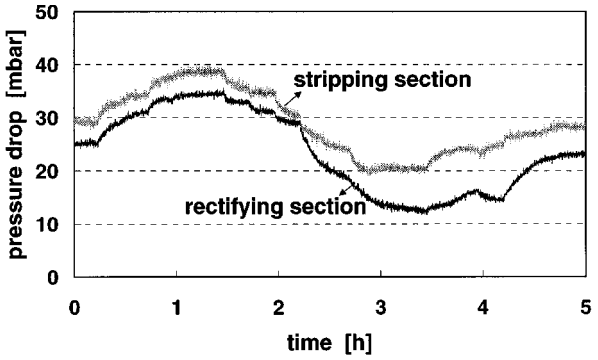


**Figure 18. Measured trajectories of the pressure drop of the rectifying and the stripping section.**

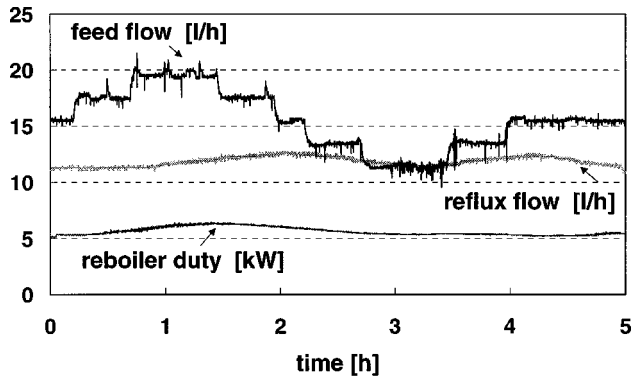


**Figure 19. Reflux flow and reboiler duty resulting from the PID controllers and the implemented feed flow.**

periment shows that due to the tray hydraulics, a bottom temperature control with a fixed set point is not proper for column operation, if the feed flow changes significantly.

## Conclusions

In this work we considered a new process optimization problem under uncertainty, that is, the operation of distillation processes with uncertain feedstreams coming from upstream plants. These flows are very different during the days from those in the night, and during the normal working days from those at the weekends. These changing streams cause undesired tank operations, as well as significant changes of the operating point of the downstream distillation column. A novel strategy composed of a stochastic optimization under chance constraints and a deterministic dynamic optimization was proposed to solve such operation problems. The stochastic information of the feedstreams was employed to receive an optimal planning for the process operation by developing a flat feed policy to the column, while allowing the tank level to change inside the required region with a predefined probability. The feasibility analysis for the stochastic optimization problem was made and an easy-to-use method was proposed to compute the maximum reachable probability of holding the constraints. This leads to a guarantee to obtain a feasible solution of the chance constrained stochastic problem, which is especially important for an online optimization of such processes.

The deterministic optimization is carried out for the operation of the downstream column under the feed policy from the stochastic optimization. This leads to a nonlinear large-scale dynamic optimization problem that is solved by a sequential approach. The proposed strategy as a whole presents an appropriate example of integration of optimization and control. The realization of the optimal policies on a pilot plant demonstrate the proposed approach. It takes about 2 min and 10 min CPU-time for a run of the stochastic and deterministic optimization by using a SUN Ultra1 Station (143 MHz), respectively.

A straightforward extension of the present work is the online optimization of such processes. An online optimization demands computationally a higher robustness and a high efficiency. Furthermore, a state observer should be developed for predicting the unmeasured state variables such as composition on each tray of the column. These will be used for the prediction of the initial state of the future horizon. An on-line parameter updating (such as the tray efficiency) via a real-time identification is also required for an adaptive framework.

Moreover, we will extend the approach to optimal operation under *uncertain compositions* of the feed flows. This is also a usual case in the process industry which has considerable effects on the operation of the downstream plants. A study on the influence of oscillations of feed composition on the operating energy should be made, so that a suitable problem can be defined. Since the only controllable stream is the outflow from the tank, optimization may result in a compensation of the smoothness between its flow rate and composition. The reason is twofold for our choice to consider only flow rate as uncertain variables in this work. First, cases of overflow and an empty feed tank appear frequently in the industrial plant, and these are directly caused by the uncertain flow rates from the upstream plants. Second, introducing inflow composition as uncertain variables will lead to a *nonlinear* stochastic optimization problem under chance constraints. A method to address this problem is being studied (Wendt et al., 2001b).

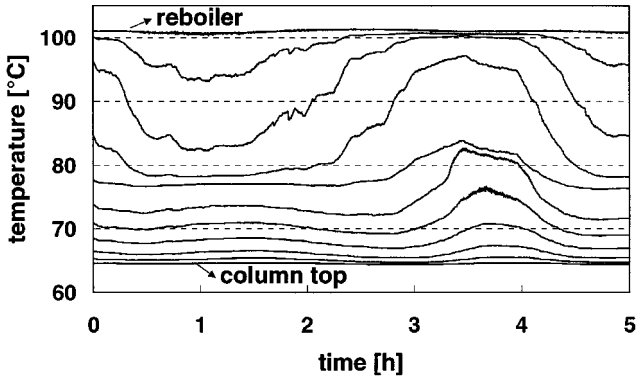


**Figure 20. Measured temperature trajectories in the condenser, of every two trays in the column, and in the reboiler by PID-control.**

## Acknowledgments

We thank Deutsche Forschungsgemeinschaft (DFG) for the financial support from the program "Echtzeit-Optimierung gro$\beta$er Systeme". W. Römisch from Humboldt Universität zu Berlin, and R. Henrion and A. Möller from Weierstra$\beta$-Institut für Angewandte Analysis und Stochastik, Berlin are gratefully acknowledged for their constructive discussions on the stochastic methods during this work.

## Literature Cited

Acevedo, J., and E. N. Pistikopoulos, "Stochastic Optimization Based Algorithms for Process Synthesis under Uncertainty," *Comput. Chem. Eng.*, **22**, 647 (1998).

Ahmed, S., and N. V. Sahinidis, "Robust Process Planning under Uncertainty," *Ind. Eng. Chem. Res.*, **37**, 1883 (1998).

Arellano-Garcia, H., R. Henrion, P. Li, A. Möller, W. Römisch, M. Wendt, and G. Wozny, "A Model for the On-line Optimization of Integrated Distillation Columns under Stochastic Constraints," DFG-Schwerpunktprogramm "Echtzeit-Optimierung grosser Systeme," Preprint 98-32 (1998).

Bernado, F. P., E. N. Pistikopoulos, and P. M. Saraiva, "Integration and Computational Issues in Stochastic Design and Planning Optimization Problems," *Ind. Eng. Chem. Res.*, **38**, 3056 (1999).
Bhatia, T., and L. T. Biegler, "Dynamic Optimization for Batch Design and Scheduling with Process Model Uncertainty," *Ind. Eng. Chem. Res.*, **36**, 3708 (1997).
Cervantes, A., and L. T. Biegler, "Large-scale DAE Optimization Using a Simultaneous NLP Formulation," *AIChE J.*, **44**, 1038 (1998).
Clay, R. L., and I. E. Grossmann, "A Disaggregation Algorithm for the Optimization of Stochastic Planning Models," *Comp. Chem. Eng.*, **21**, 751 (1997).
Diwekar, U. M., and E. S. Rubin, "Stochastic Modeling of Chemical Processes," *Comp. Chem. Eng.*, **15**, 105 (1991).
Diwekar, U. M., and J. R. Kalagnanam, "Efficient Sampling Technique for Optimization under Uncertainty," *AIChE J.*, **43**, 440 (1997).
Feehery, W. F., and P. I. Barton, "Dynamic Optimization with State Variable Path Constraints," *Comp. Chem. Eng.*, **22**, 1241 (1998).
Gill, P. E., W. Murray, and M. A. Saunders, "SNOPT: An SQP Algorithm for Large-scale Constrained Optimization," Report NA 97-2, Department of Mathematics, University of California, San Diego (1997).
Gill, P. E., W. Murray, and M. A. Saunders, "User's Guide for SNOPT 5.3: A FORTRAN Package for Large-scale Nonlinear Programming," Report NA 97-3, Dept. of Mathematics, University of California, San Diego (1997).
Gmehling, J., U. Onken, and W. Arlt, VLE Data Collection, DECHEMA, Frankfurt (1977).
Gupta, A., and C. D. Maranas, "A Two-Stage Modeling and Solution Framework for Multiside Midterm Planning under Demand Uncertainty," *Ind. Eng. Chem. Res.*, **39**, 3799 (2000).
Halemane, K. P., and I. E. Grossmann, "Optimal Process Design under Uncertainty," *AIChE J.*, **29**, 425 (1983).
Henrion, R., and W. Römisch, "Metric Regularity and Quantitative Stability in Stochastic Programs with Probabilistic Constraints," *Mathematical Programming*, **84**, 55 (1999).
Kall, P., and S. W. Wallace, *Stochastic Programming*, Wiley, New York (1994).
Leineweber, D. B., H. G. Bock, and J. P. Schröder, "Fast Direct Methods for Real-Time Optimization of Chemical Processes," *Proc. of 15th IMACS World Congress on Scientific Computation*, A. Sydow, ed., Modeling and Applied Mathematics, **6**, 451 (1997).
Li, P., "Entwicklung optimaler Führungsstrategien für Batch-Destillationsprozesse," Fortschritt-Berichte VDI, Reihe 3, Nr. 560 (1998).
Li, P., H. Arellano-Garcia, G. Wozny, and E. Reuter, "Optimization of a Semibatch Distillation Process with Model Validation on the Industrial Site," *Ind. Eng. Chem. Res.*, **37**, 1341 (1998).
Li, P., M. Wendt, and G. Wozny, "Probabilistically Constrained Generalized Predictive Control," *Proc. of ADCHEM 2000*, Pisa, Italy, 14-16.06, 1007 (2000a).
Li, P., M. Wendt, and G. Wozny, "Robust Model Predictive Control under Chance Constraints," *Comp. Chem. Eng.*, **24**, 829 (2000b).
Liu, M. L., and N. V. Sahinidis, "Optimization in Process Planning under Uncertainty," *Ind. Eng. Chem. Res.*, **35**, 4154 (1996).
Logsdon, J. S., and L. T. Biegler, "Accurate Determination of Optimal Reflux Policies for the Maximum Distillate Problem in Batch Distillation," *Ind. Eng. Chem. Res.*, **28**, 1628 (1989).
Logsdon, J. S., and L. T. Biegler, "Decomposition Strategies for Large-scale Dynamic Optimization Problems," *Chem. Eng. Sci.*, **47**, 851 (1992).
Loeve, M., *Probability Theory*, Van Nostrand-Reinhold, Princeton, NJ (1963).
Papoulis, A., *Probability, Random Variables and Stochastic Processes*, McGraw-Hill, New York (1965).
Pistikopoulos, E. N., and M. G. Ierapetritou, "Novel Approach for Optimal Process Design under Uncertainty," *Comp. Chem. Eng.*, **19**, 1089 (1995).
Prékopa, A., *Stochastic Programming*, Kluwer, Dordrecht, The Netherlands (1995).
Reid, R. C., J. M. Prausnitz, and B. E. Poling, *The Properties of Gases and Liquids*, McGraw-Hill, New York (1987).
Rooney, W. C., and L. T. Biegler, "Incorporating Joint Confidence Regions into Design under Uncertainty," *Comp. Chem. Eng.*, **23**, 1563 (1999).
Schwarm, A. T., and M. Nikolaou, "Chance-constrained Model Predictive Control," *AIChE J.*, **45**, 1743 (1999).
Steinbach, M., "Fast Recursive SQP Methods for Large-scale Optimal Control Problems," PhD Diss., Universität Heidelberg, Preprint 95-27 (1995).
Subrahmanyam, S., J. F. Pekny, and G. V. Reklaitis, "Design of Batch Chemical Plants under Market Uncertainty," *Ind. Eng. Chem. Res.*, **33**, 2688 (1994).
Szántai, T., "A Computer Code for Solution of Probabilistic-constrained Stochastic Programming Problems," *Numerical Techniques for Stochastic Optimization*, Y. Ermolive and R. J.-B. Wets, eds., Springer-Verlag, New York, p. 229 (1988).
Torvi, H., and T. Herzberg, "Estimation of Uncertainty in Dynamic Simulation Results," *Comput. Chem. Eng.*, **21** (Suppl.), S181 (1997).
Varvarezos, D. K., I. E. Grossmann, and L. T. Biegler, "An Outer-Approximation Method for Multiperiod Design Optimization," *Ind. Eng. Chem. Res.*, **31**, 1466 (1992).
Vassiliadis, V. S., C. C. Pantelides, and R. W. H. Sargent, "Solution of a Class of Multistage Dynamic Optimization Problems, 1. Problems without Path Constraints," *Ind. Eng. Chem. Res.*, **33**, 2111 (1994).
Wendt, M., P. Li, and G. Wozny, "Batch Distillation Optimization with a Multiple Time-Scale Sequential Approach for Strong Nonlinear Processes," *Proc. of ESCAPE-10*, S. Pierucci, ed., *Computer-Aided Chemical Engineering*, **8**, 121 (2000).
Wendt, M., P. Li, and G. Wozny, "Model Parameter Updating for Large-scale Dynamic Nonlinear Processes by On-line Simulation and Optimization," presented at the 3rd Eur. Congress of Chem. Eng., Nuremberg, June 26–28, 2001 (2001a).
Wendt, M., P. Li, and G. Wozny, "Nonlinear Chance Constrained Process Optimization under Uncertainty," *Ing. Eng. Chem. Res.*, submitted (2001b).
Wozny, G., and P. Li, "Planning and Optimization of Dynamic Plant Operation," *Appl. Thermal Eng.*, **20**, 1393 (2000).

## Appendix: Theorem for the Maximal Joint Probability of a Multivariate Normal Distribution

*Theorem:* For a multivariate normal distribution the maximal value of the joint probability is achieved, if

$$\mu_{y(i)} = \frac{y_{\min} + y_{\max}}{2} \qquad i = 1, \cdots, N \tag{A1}$$

*Proof:* Let the probability density function of the output vector be

$$\varphi_N(\boldsymbol{y}) = \frac{1}{|\boldsymbol{R}_y|^{1/2}(2\pi)^{N/2}} e^{-\frac{1}{2}(\boldsymbol{y}-\boldsymbol{\mu}_y)^T \boldsymbol{R}_y^{-1}(\boldsymbol{y}-\boldsymbol{\mu}_y)} = \gamma e^{f(\boldsymbol{y})} \tag{A2}$$

where $\gamma$ and $f(\boldsymbol{y})$ are the corresponding constant and function, respectively. The joint probability means

$$P(\boldsymbol{\mu}_y) = \int_{y_{\min}}^{y_{\max}} \cdots \int_{y_{\min}}^{y_{\max}} \cdots \int_{y_{\min}}^{y_{\max}} \varphi_N(\boldsymbol{y}) dy(1) \cdots dy(i) \cdots dy(N) \tag{A3}$$

at the maximum point, there will be

$$\frac{\partial P(\boldsymbol{\mu}_y)}{\partial \mu_y(i)} = 0 \qquad i = 1, \cdots, N \tag{A4}$$

Since

$$\frac{\partial \varphi_N(\boldsymbol{y})}{\partial \mu_y(i)} = \gamma e^{f(\boldsymbol{y})} \frac{\partial f(\boldsymbol{y})}{\partial \mu_y(i)} \tag{A5}$$

From Eq. A2

$$\frac{\partial f(\mathbf{y})}{\partial \mu_y(i)} = -\frac{\partial f(\mathbf{y})}{\partial y(i)} \tag{A6}$$

From Eq. A3 and Eq. A4 we have

$$\int_{y_{\min}}^{y_{\max}} \cdots \int_{y_{\min}}^{y_{\max}} \left[ \int_{y_{\min}}^{y_{\max}} \gamma e^{f(y)} df(\mathbf{y}) \right]_i \times dy(1) \cdots dy(i-1) dy(i+1) \cdots dy(N) = 0 \tag{A7}$$

That is

$$\int_{y_{\min}}^{y_{\max}} \cdots \int_{y_{\min}}^{y_{\max}} \int_{y_{\min}}^{y_{\max}} \cdots \int_{y_{\min}}^{y_{\max}} \varphi_{N-1}[y(1), \cdots, y(i-1) \; y(i+1), \cdots, y(N)]_{y(i)=y_{\min}} dy(1) \cdots dy(i-1) dy(i+1) \cdots dy(N)$$

$$= \int_{y_{\min}}^{y_{\max}} \cdots \int_{y_{\min}}^{y_{\max}} \int_{y_{\min}}^{y_{\max}} \cdots \int_{y_{\min}}^{y_{\max}} \varphi_{N-1}[y(1), \cdots, y(i-1) \; y(i+1) \cdots, y(N)]_{y(i)=y_{\max}} dy(1) \cdots dy(i-1) dy(i+1) \cdots dy(N) \tag{A8}$$

It means

$$\Phi_{N-1}[y(1), \cdots, y(i-1), y(i+1), \cdots y(N)]_{y(i)=y_{\min}} = \Phi_{N-1}[y(1), \cdots, y(i-1), y(i+1), \cdots y(N)]_{y(i)=y_{\max}} \tag{A9}$$

Since $\Phi_{N-1}$ is the probability function of $N-1$ joint events of normally distributed variables, it is continuous and symmetric. Since $y_{\min} \neq y_{\max}$, then the mean of $y(i)$ must be at the center of $[y_{\min}, y_{\max}]$.

*Manuscript received Aug. 7, 2000, and revision received June 4, 2001.*